Improved acoustic performance simulation for hollow brick walls

Simon Bailhache, Sébastien Ciukaj, Thibaut Blinet, Catherine Guigou-Carter

IMPROVED ACOUSTIC PERFORMANCE SIMULATION FOR HOLLOW BRICK WALLS

Simon Bailhache[1] Sébastien Ciukaj[2] Thibaut Blinet[3] Catherine Guigou-Carter[1]

[1] CSTB, 24 rue Joseph Fourier, 38400 Saint-Martin-d'Hères, France

[2] CTMNC, 200 avenue du Général De Gaulle, 92140 Clamart, France

[3] CSTB, 84 avenue Jean Jaurès, 77420 Champs-sur-Marne, France

Simon.bailhache@cstb.fr

ABSTRACT

This study aims at improving the prediction of the sound transmission loss performance of fired clay hollow brick walls, with or without a thermal lining, using a finite-size transfer matrix method (FTMM). The hollow brick layer is described as a thick, homogeneous, anisotropic plate. The physical properties of the equivalent material are obtained by means a static homogenization process based on a finite element method. This initial step considers a variable horizontal offset between successive rows of bricks and the frequency range of the specific Lamb mode behavior, driven by the stiffness of the wall thickness. Therefore, a range of values is obtained for each of the elastic parameters of the anisotropic material. Then, these variation ranges are used as boundary conditions for an automatic model fitting based on a genetic algorithm coupled to the FTMM prediction tool. Then, the model of the brick wall is used in new predictions on a large scope of brick geometries including also different types of thermal linings. The presence of mortar dabs distributed over the wall surface is accounted for by means of an analytical approach developed in previous work and implemented in the prediction tool. Measurement and prediction results are presented in terms of sound reduction index of the bare walls and sound reduction index improvement of the linings.

1. INTRODUCTION

Nowadays, the use of prediction software to simulate the acoustic performance of fired clay hollow brick walls is still associated to limited accuracy.

One of the difficulties is the anisotropic behavior of the bricks which needs specific models and reliable input data. This anisotropic behavior is often studied at the scale of a single brick, which cannot always represent the behavior of the entire wall due to the presence of a (variable) horizontal offset between successive rows. Section 2 of this paper presents a method to integrate the effect of this offset in the physical description of the wall. The mechanical parameters of the brick layer are considered as variable within a given range. Automatic optimization coupled to a finite-size transfer matrix method (FTMM) prediction tool is used to determine a set of parameters that best matches the measured acoustic performance.

Another difficulty is that such walls are often associated to interior linings attached by means of mortar dabs regularly distributed over the wall surface. This partial contact condition is often not considered by FTMM-based tools which can deal with ideal contacts – either fully free or fully glued. In a previous study, an analytical approach was proposed to model this partial contact and applied to a concrete supporting wall. In the present work, the same approach is applied to the optimized models of fired clay hollow brick walls, considering different types of linings. Prediction and measurement results are presented in Section 3 of this paper. This analytical approach was implemented in the latest version of CSTB's AcouSYS software.

2. BARE BRICK WALLS WITH COATING

2.1 Limits of Previous Modelling Attempts

In the past years, different approaches were proposed to account for the anisotropic behavior of hollow clay bricks in acoustic performance predictions. While Finite Element Methods (FEM) can help understand the physical phenomena driving the performance, they are still limited in terms of frequency range and may not be adapted for engineering purposes.

Jacqus et al. [1] proposed an approach based on the homogenization of the bricks, considering that they are stacked on top of each other. The equivalent homogeneous, orthotropic material can then be used in FTMM-based predictions, thus allowing to cover the entire frequency range considered in building acoustics within reasonable computation time. However, the accuracy of the prediction results is not always satisfactory and may require fitting the model – e.g. by tuning the mechanical properties and/or the loss factor manually [2-3].

More recently, Granzotto et al. [4] proposed an analytical method based on Cremer's theory, also using the mechanical properties of a single brick as input data. No account of the offset between rows of bricks is taken. Predicted and measured results show good agreement between 250 Hz and 2500 Hz, but some discrepancies are observed in the low and high frequency ranges.

In the present work, the offset between rows of bricks is taken into account by defining variation ranges for the

orthotropic properties of the brick layer. To this end, a FEM-based static optimization is performed (see section 2.2). Minimum and maximum values for each parameter are then used as limits to fit a FTMM model of the coated wall, by means of an automatic genetic-based optimization tool (see section 2.3). This approach is applied to 10 different fired clay hollow brick walls from the 3 main manufacturers in France, covering a wide range of structural geometries. Prediction results are then compared to the sound reduction index measured in the laboratory. Results are presented in section 2.4.

2.2 Offset-dependent Wall Properties

The method presented below consists in identifying the equivalent orthotropic elastic parameters of a hollow building element such as a brick masonry with vertical perforations, like the fictitious element shown in Fig 1. These equivalent parameters are obtained by a numerical homogenization calculation, the boundary conditions taking into account the non-superposed assembly of bricks in a traditional masonry wall.

These boundary conditions for the lower and the upper faces of a brick are induced by the longitudinal offset of the elements between two successive rows of bricks. It is the superposition of the geometrical partitions of bricks that ensures the structural continuity and the vertical stiffness of the structure, also depending on the contact areas, as shown in blue in Fig. 1 and Fig. 2.

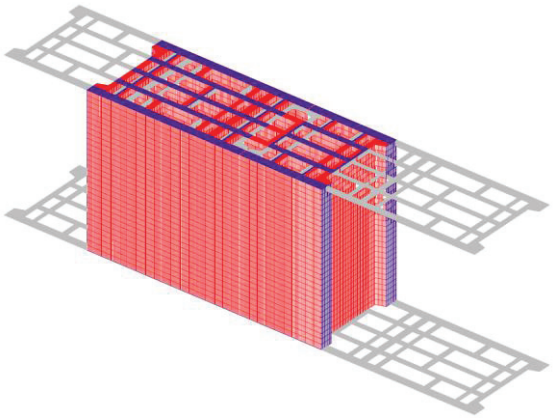

Figure 1. 3D representation of the fictitious element with the footprint of the upper and the lower masonry rows in grey, above and below the element.

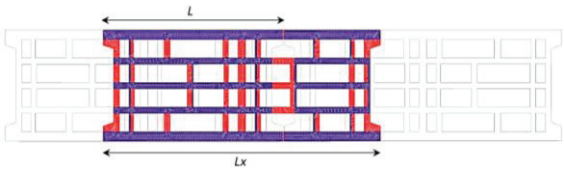

Figure 2. 2D representation of the fictitious element with, in blue, the contact area $S_{contact}$ with the upper and the lower masonry rows, and in red, the free area S_{free} (without contact).

The evolution of the function $K = f(L / Lx)$ is shown for the fictitious element on the graph in Fig. 3. K is defined by the $S_{contact} / S_{brick}$ ratio, with $S_{brick} = S_{contact} + S_{free}$. L is the absolute longitudinal offset between successive rows of brick, with $L / Lx \in [0.33; 0.66]$ (blue line in Fig. 3), Lx being the constant length of the element. The K function is studied for 3 bricks manufactured in France, called in this paper brick A, brick B and brick C.

Then, the extrema K_{min} and K_{max} are determined and the corresponding boundary conditions are considered for numerical homogenization tests on the alveolar element. This step aims at determining variation ranges for the elastic properties of the equivalent homogeneous material, and in particular for the E_z, G_{xz} and G_{yz} modules.

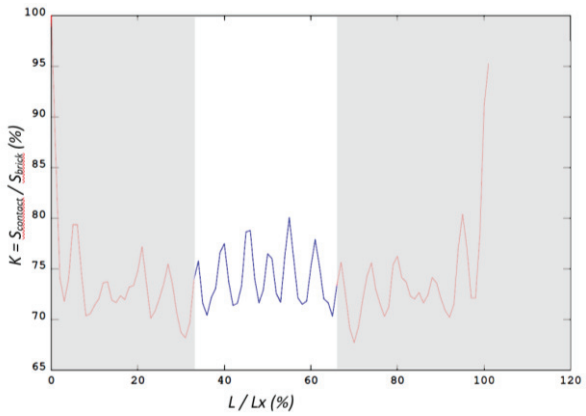

Figure 3. Graph of K function for the determination of K_{min} and K_{max} positions.

The numerical homogenization tests shown in Fig. 4, are carried out according to a finite element method defined in the linear domain with 3D volume meshes.

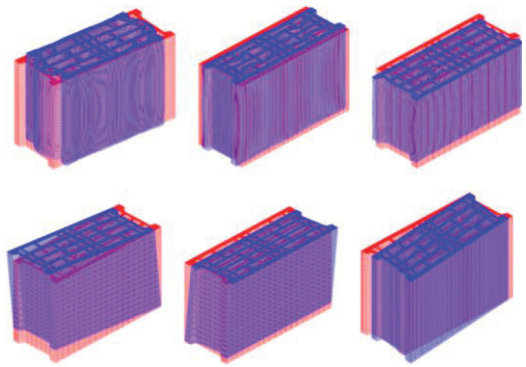

Figure 4. Undeformed meshes in red and deformed meshes in blue for numerical test of homogenization of E_x, E_y, E_z (also ν_{yz}, ν_{xz}, ν_{xy}) on top and G_{xz}, G_{yz}, G_{xy} on bottom.

Two isotropic Young moduli are beforehand defined for the fired clay material, by iteration of homogenization tests until converging to the criterion dictated by [1] for the Lamb S1 mode frequency targeting each bound of the one-third octave band which is corresponding to the acoustic

attenuation dip near 2 kHz of the sound transmission loss curve measured in laboratory for 20 cm thick bricks.

This process allows to obtain for each brick, two sets of 9 extremum orthotropic elastic parameters, which can then be considered as limits for the genetic algorithm used to fit the acoustic prediction model.

2.3 Automatic Model Fitting

For each considered wall, FTMM simulations of the sound reduction index are performed and compared to the results of laboratory measurements. In these simulations, the wall is described as a two-layer system. The hollow brick layer has variable mechanical properties within the ranges defined in Section 2.2. The coating layer is described as a solid isotropic material, with fixed mechanical properties. An automatic optimization tool based on a genetic algorithm is used to determine a set of optimized parameters for the brick layer, which gives the minimum difference between predicted and measured acoustic performance over a specified frequency range.

For each individual, the 3 Young moduli E_x, E_y and E_z as well as the 3 shear moduli G_{xy}, G_{yz} and G_{zx} are considered as variable, while the Poisson coefficients are automatically updated so that the following elasticity relations remain valid:

$$\upsilon_{xy} E_y = \upsilon_{yx} E_x \quad (1)$$

$$\upsilon_{xz} E_z = \upsilon_{zx} E_x \quad (2)$$

$$\upsilon_{yz} E_z = \upsilon_{zy} E_y \quad (3)$$

Finally, the loss factor of the brick layer is adjusted manually to further reduce the errors between predictions and measurements of the sound reduction index.

As it is assumed that the low frequency performance is driven by physical phenomena not considered by the FTMM (modal behavior), the whole model fitting approach is performed twice and independently for separate frequency domains. First, the critical frequencies of the brick layer in both directions $f_{c,x}$ and $f_{c,y}$ are calculated from the mechanical properties of the brick layer (minimum values). The transition frequency between the two frequency domains is then obtained according to Eqn. (4).

$$f_t = \sqrt{f_{c,x} \times f_{c,y}} \quad (4)$$

Then, two automatic optimizations are performed independently. For one-third octave bands having their center frequency above f_t, the limits considered for the Young and shear moduli by the algorithm are the minimum and maximum values determined as in Section 2.2. For one-third octave bands with a center frequency below f_t, extended limits are considered (minimum divided by 25, maximum multiplied by 25).

Therefore, the brick layer is associated to 2 independent sets of mechanical properties. In principle, however, Poisson coefficients are constant with frequency. Thus, it is chosen to use the Poisson coefficient values determined in the medium-high frequency domain to ensure physical consistency at least in the frequency range where the FTMM approach is considered as relevant.

2.4 Results

Due to paper length limitation, results are presented here for only 3 of 10 brick walls. The transition frequencies calculated according to Eqn. (4) for the 3 brick layers are shown in Tab. 1.

	f_t (Hz)
Wall A	282
Wall B	266
Wall C	223

Table 1. Transition frequency of the walls.

Fig. 5 to 7 show the elastic properties of the brick layers before and after the automatic model fitting in both frequency domains.

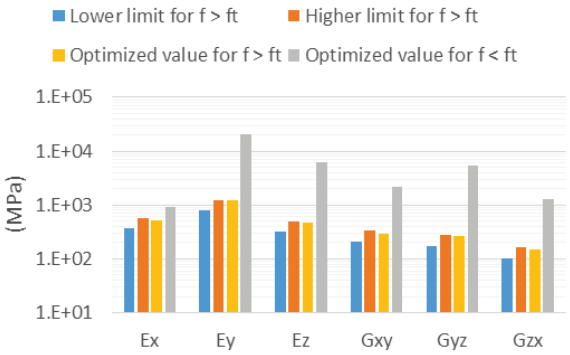

Figure 5. Elastic properties of the brick layer for wall A.

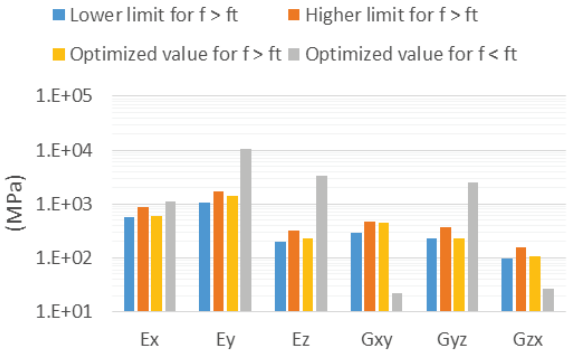

Figure 6. Elastic properties of the brick layer for wall B.

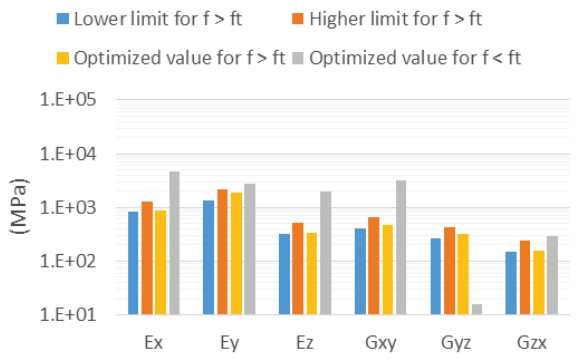

Figure 7. Elastic properties of the brick layer for wall C.

Fig. 8 to 10 show the measured sound reduction index spectra together with 2 different prediction results: (1) with the optimized elastic parameters but a constant loss factor of 0.03, and (2) with the optimized elastic parameters and a manually adjusted (frequency-dependent) loss factor.

It can be observed that the predictions with a constant loss factor give close results to the experimental values regarding the ISO 717-1 single number ratings. However, when it comes to spectral values, bigger deviations are observed. These deviations can be compensated by adjusting the loss factor, with predicted acoustic performance within 2 dB of the experimental values – except a 3.5 dB gap at 100 Hz for wall C.

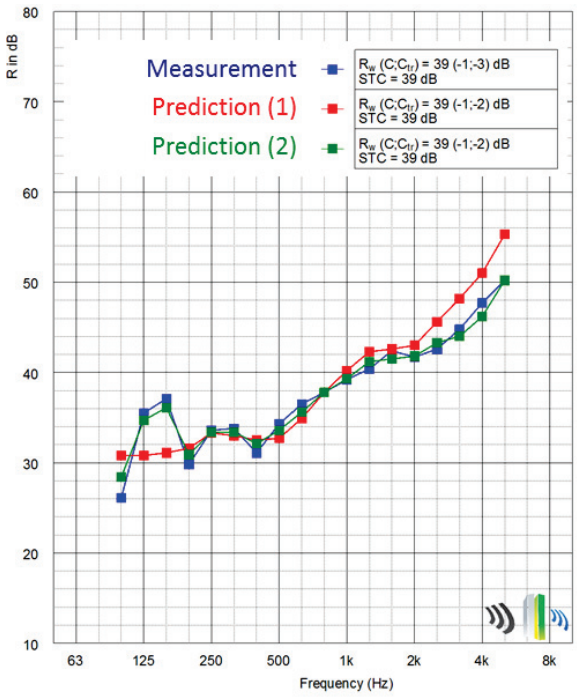

Figure 8. Sound reduction index R of wall A (coated on one side).

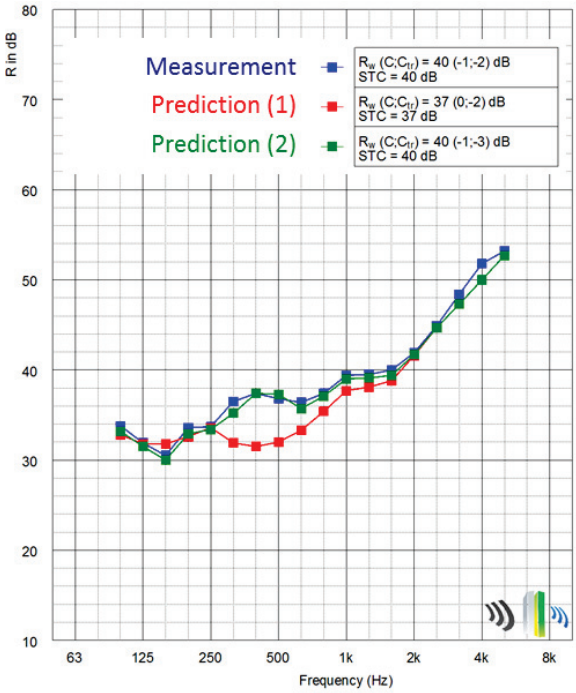

Figure 9. Sound reduction index R of wall B (coated on one side).

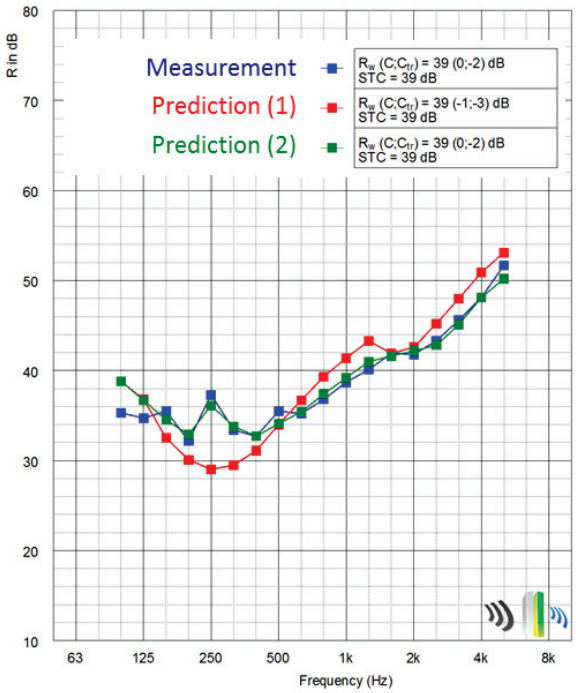

Figure 10. Sound reduction index R of wall C (coated on one side).

3. BRICK WALLS WITH THERMAL LININGS

3.1 Analytical model

In 2016, an analytical method was proposed to consider the influence of mortar dabs when predicting the sound reduction index of walls equipped with a thermal lining

[6]. This method uses an equivalent spring representation of the system, with specific models depending on the type of insulating material – either closed-cell foams (considered as isotropic solids) or open-cell foams or fibrous materials (considered as porous). This previous study considered only a solid concrete wall as supporting element. The equivalent spring is modelled by a fictitious air layer, with an adapted thickness, placed between the base wall and the insulating material. The air layer thickness depends in particular on the dynamic stiffness of the insulating material and on the dabs bonding rate (after compression). For porous insulating materials, it is also proposed to use a different method based on an equivalent porous model, without any air layer. This approach gave the closest results to the measured lining performance ΔR in low frequencies (up to 250 Hz) for the case considering a concrete wall.

In the present work, the same approach is applied to the 10 hollow brick walls under study, each one being associated to several linings. Only a few cases are covered in this paper.

For porous insulating materials, the equivalent porous model is considered. For closed-cell materials, the fictitious air layer model is modified by applying a constant loss factor of 0.25 to this air layer, considering higher damping in the cavity in the case of fired clay bricks (with a porous surface) than with concrete. Both modelling approaches are implemented in version 4 of AcouSYS [7].

3.2 Input parameters

This part of the work considers the optimized mechanical parameters for the supporting hollow brick wall with its exterior coating. The linings are described as 2 layers in glued contact, i.e. the insulating material and a gypsum board.

Most of the linings considered in this study were characterized in the laboratory. In particular, measured values are available for the dynamic stiffness and loss factor of the insulating materials, as well as for the density of the gypsum boards. For the other parameters – e.g. elastic properties of the gypsum boards, airflow resistivity of mineral wools – typical values are used.

The dab bonding rate is calculated from the following mounting-related parameters, which are documented in the measurement test reports:

- Number of dabs per m²: 9.3;
- Diameter of the dabs before compression: 100 mm for closed-cell foams, 130 mm for mineral wools;
- Thickness of the dabs before compression: 15 mm;
- Thickness of the dabs after compression: 10 mm.

It should be noted that the values of these lining-related parameters were not questioned in this study, even though they are definitely associated to uncertainties that could explain differences between predicted and measured results.

3.3 Results

Two examples are considered in this section, one with a closed-cell insulating material and the other one with a fibrous insulating material.

The first system is composed of wall A (coated on one side) equipped with a thermal lining made of 80 mm thick expanded polystyrene (EPS) and a 9.5 mm thick standard gypsum board. The Young modulus of the EPS layer derived from its measured dynamic stiffness is 2.940 MPa.

Three different modelling approaches are tested:

- A simple multilayer system where the dabs are neglected, and the EPS layer is considered fully glued to the brick wall;
- Another simple multilayer system where the dabs are neglected, and the EPS layer is considered fully free from the brick wall;
- A multilayer with the dabs modelled using the fictitious damped air layer.

The sound reduction index of the lined wall is represented in Fig. 11. The sound reduction index improvement of the lining is represented in Fig. 12.

These results show a good agreement – up to 1600 Hz – between the measured performance and the transmission loss predicted with the dabs taken into account. At higher frequencies however, significant deviations are observed. The single number ratings being mostly determined by the low and mid frequency behavior, the $\Delta(R_w + C)_{direct}$ and $\Delta(R_w + C_{tr})_{direct}$ values of the lining are the same according to the prediction and the measurement.

In contrast, the two simpler models with either glued or free contact between the support wall and the lining seem more accurate in the high frequency range. This comes at the expense of big deviations between 200 and 630 Hz, where a mass-spring-mass behavior results in negative predicted ΔR values while the measured performance is close to 0 dB.

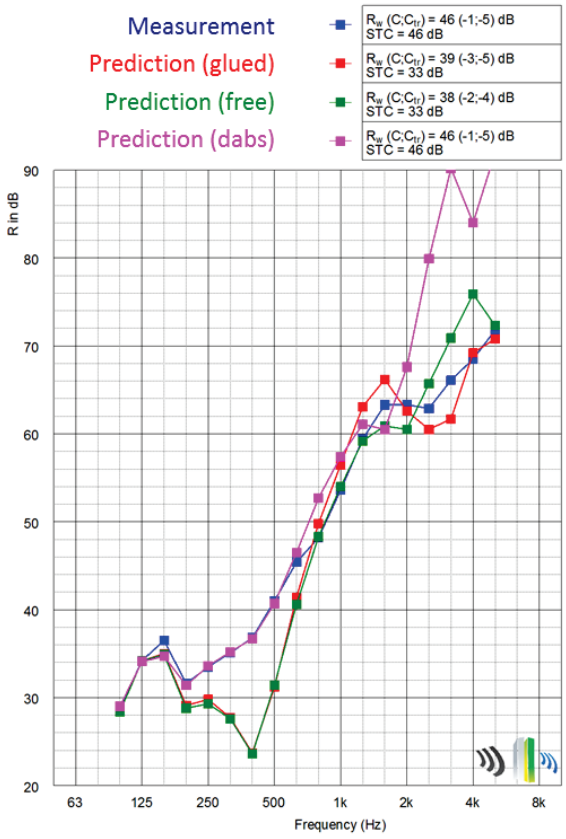

Figure 11. Sound reduction index R of wall A with an EPS-based thermal lining.

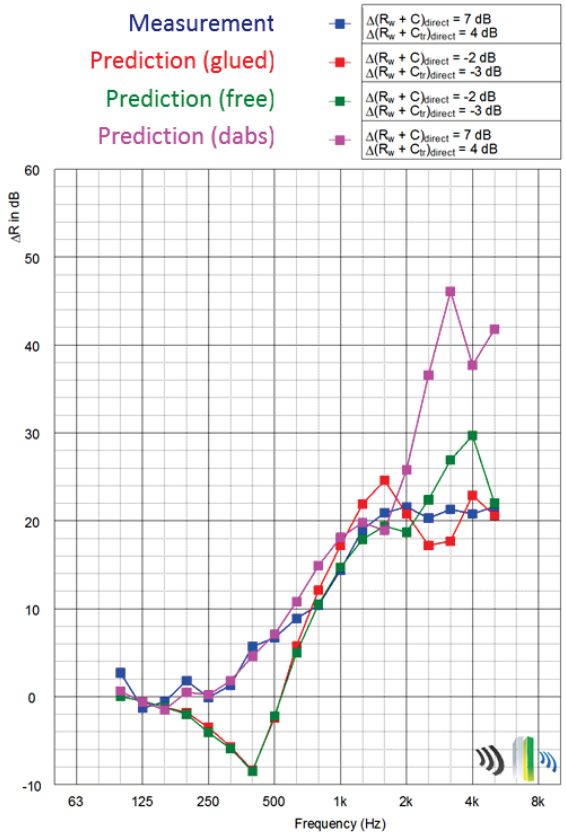

Figure 12. Sound reduction index improvement ΔR of an EPS-based thermal lining associated to wall A.

The second system is composed of wall B (coated on one side) equipped with a thermal lining made of 100 mm thick stone wool and a 9.5 mm thick standard gypsum board. The mineral wool layer is modeled as a poroelastic material. The Young's modulus of its skeleton, derived from its measured dynamic stiffness, is 0.254 MPa.

Three different modelling approaches are tested:

- A simple multilayer system where the dabs are neglected, and the stone wool layer is considered fully glued to the brick wall;
- Another simple multilayer system where the dabs are neglected, and the stone wool layer is considered fully free from the brick wall;
- A multilayer with the dabs modelled using the equivalent porous layer (combining the air, dabs and stone wool layer).

The sound reduction index of the lined wall is represented in Fig. 13. The sound reduction index improvement of the lining is represented in Fig. 14.

These results show that the interest of the equivalent porous approach is limited to the lower frequency bands, as it was previously observed with a concrete support wall. From 250 Hz, the predicted performance strongly overestimates the experimental values. In terms of single number ratings, $\Delta(R_w + C)_{direct}$ and $\Delta(R_w + C_{tr})_{direct}$ values of the lining are overestimated by 1 dB only.

When neglecting the influence of the dabs and under a fully glued contact condition, the predicted results are much lower than the experimental values, in particular at low frequencies where an important performance dip is obtained due to the mass-spring-mass resonance of the system.

Prediction results with a free contact condition are in very good agreement with the measured values up to 500 Hz. The same observation is obtained for other associations of hollow brick walls and fibrous insulating materials. Therefore, this approach appears to be more relevant for such systems, even though the acoustic performance is again overestimated at higher frequencies. In terms of single number ratings, for this particular system, an underestimation of 1 dB is obtained for the $\Delta(R_w + C)_{direct}$ performance of the lining, while $\Delta(R_w + C_{tr})_{direct}$ values are the same according to the prediction and the measurement.

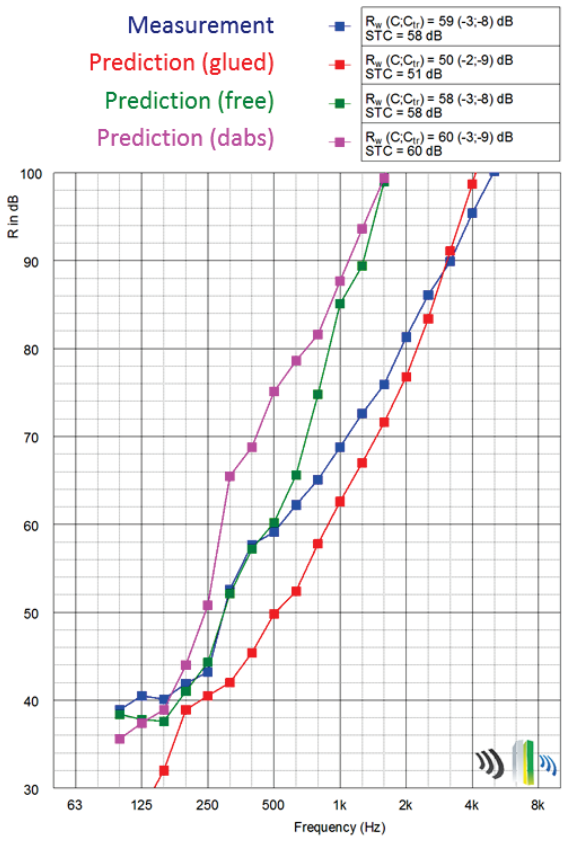

Figure 13. Sound reduction index R of wall B with a mineral wool-based thermal lining.

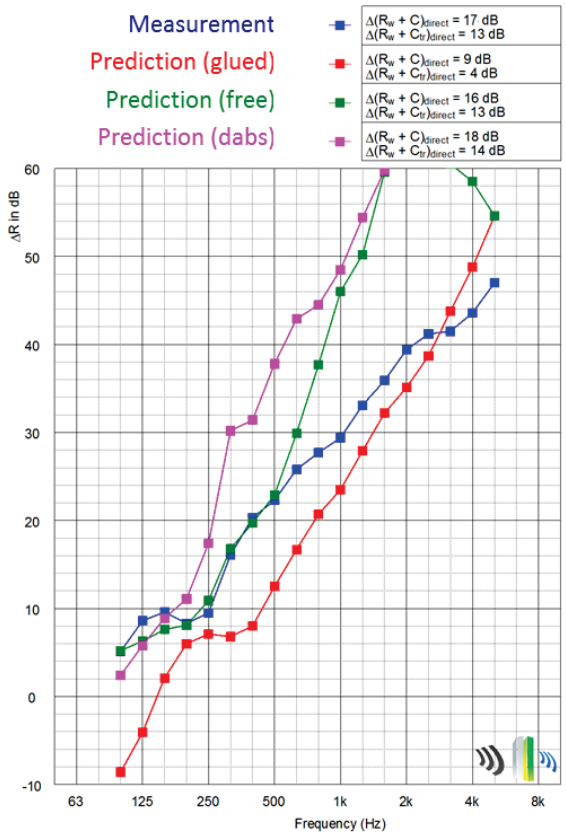

Figure 14. Sound reduction index improvement ΔR of a mineral wool-based thermal lining associated to wall B.

4. CONCLUSIONS

In this study, the sound reduction index of fired clay hollow brick walls was predicted using a FTMM approach. The equivalent orthotropic solid material properties used to model the brick layer were determined in three steps. First, variation ranges were defined for the elastic parameters, through a numerical static optimization considering a variable lateral offset between successive rows of bricks. In a second step, these ranges were used as boundaries in a genetic algorithm coupled to the FTMM prediction software to determine optimum mechanical properties that allow minimizing the difference between predicted and measured acoustic performances. This automatic model fitting approach allowed to obtain rather reasonably accurate models. Finally, a third step consisted in adjusting the loss factor of the brick layer manually, to compensate the remaining deviations.

The whole procedure was applied to 10 different walls and representative results are presented in this paper for 3 of them. These results show a good agreement between predicted and measured acoustic performances, regarding both spectral values and single number ratings calculated according to ISO 717-1.

One limitation of this approach is that specific values were defined for the elastic parameters of the brick layer at low frequencies (up to 250 Hz on average), where the acoustic performance is driven by structural modes. Therefore, the physical consistency of the model (relations given by Equations (1) to (3) between Young moduli and Poisson coefficients) is not respected in this frequency range.

In a second part of this work, the models were modified to include thermal linings bonded by dabs. The partial contact condition introduced by the presence of the mortar dabs was taken into account by implementing an analytical method proposed in a previous study [6]. This approach was compared to simpler approaches where the dabs are neglected, considering either a free or a glued contact condition between the brick layer and the insulating material. To this end, the same 10 walls were considered in association with different linings, for which laboratory measurement results were available. Only 2 representative results are presented in this paper.

For insulating layers made of a closed-cell foam such as EPS, the proposed analytical method that takes the dabs into account seems to give the most accurate results, in particular in the low and medium frequency ranges.

For fibrous insulating materials such as mineral wools, the proposed approach seems only relevant for low frequencies. The approach that considers a free contact condition gives more accurate results on a wider frequency range and is therefore preferred.

The analytical approaches proposed for both types of insulating materials were implemented in version 4 of CSTB's software AcouSYS.

Predictions were also used to estimate the acoustic performance of combinations of brick wall and lining for

which no measurement result was available. These extrapolations are available to AcouSYS v4 users as example projects. The predicted performances show clear categories, depending on the type on insulation material (EPS, elastified EPS or mineral wool). Surprisingly, for a given lining associated to the 10 walls, predicted $\Delta(R_w + C_{tr})_{direct}$ values vary within a 5 dB range. This observation needs to be confirmed by laboratory tests.

5. REFERENCES

[1] G. Jacqus, S. Berger, V. Gibiat, P. Jean, M. Villot, and S. Ciukaj: "A homogenized vibratory model for predicting the acoustic properties of hollow brick walls", *Journal of Sound and Vibration*, Vol. 330, pp. 3400–3409, 2011.

[2] J.-B. Chéné, C. Guigou-Carter, P. Jean, T. Blinet, and G. Jacqus: "De l'usage des techniques d'homogénéisation afin d'étendre la portée des méthodes de matrices de transfert pour la modélisation de systèmes du bâtiment : Trois techniques, trois études de cas", *Proc. CFA/VISHNO*, pp. 2391-2397, 2016.

[3] T. Blinet, C. Coguenanff, S. Bailhache, and J.-B. Chéné: *AcouSYS V3 Validation Booklet*, CSTB, 2016.

[4] N. Granzotto, A. Di Bella, and E. A. Piana: "Prediction of the sound reduction index of clay hollow brick walls", *Building Acoustics*, 2020.

[5] C. Coguenanff, and C. Guigou-Carter: "Multi-criteria optimization of a wood-based floor", *Proc. 24th International Congress on Sound and Vibration*, 2017.

[6] C. Guigou-Carter, G. Jacqus, and T. Blinet: "Acoustic performance prediction for thermal linings bounded by dabs", *Proc. 23rd International Congress on Sound and Vibration*, 2016.

[7] T. Blinet, S. Bailhache, and C. Guigou-Carter: *AcouSYS V4 Validation Booklet*, CSTB, 2020.